Solid State Communications 152 (2012) 873–877

Contents lists available at SciVerse ScienceDirect

Solid State Communications

journal homepage: www.elsevier.com/locate/ssc

First principles calculations on the effect of pressure on $SiH_4(H_2)_2$

K.V. Shanavas [*,1], H.K. Poswal, Surinder M. Sharma

High Pressure & Synchrotron Radiation Physics Division, Bhabha Atomic Research Centre, Mumbai - 400 0085, India

ARTICLE INFO

Article history:
Received 31 October 2011
Received in revised form
29 January 2012
Accepted 11 February 2012
by D.D. Sarma
Available online 16 February 2012

Keywords:
A. Molecular solid
D. Phase transitions
E. First principles
E. High pressure

ABSTRACT

The effect of pressure on the strength of H_2 covalent bond in the molecular solid $SiH_4(H_2)_2$ has been investigated using quantum molecular dynamics simulations and charge density analysis. Our calculations show, in agreement with the implications of the experimental results, that substantial elongation of H_2 bond can be achieved at low pressures, with the onset of rapid changes close to 40 GPa. Model calculations show redistribution of charge from bonding to antibonding states to be responsible for the behavior. Our computed Raman spectra confirm the dynamic exchange of hydrogen atoms speculated to be operative in SiH_4–D_2 mixture by experiments. This exchange is shown to be a three step process driven by thermal fluctuations.

1. Introduction

Possibility of observation of metallic hydrogen, as predicted by Wigner and Huntington [1], has been the topic of intense research activity over the past several decades. This state is expected to have novel properties like superconductivity, superfluidity and a quantum liquid state [2]. However, the experimental observation of metallic state has been elusive so far, requiring static pressures well beyond the limits at which reliable measurements can be made in the laboratory [3,4].

The metalization pressure is expected to be lower in hydrogen rich compounds of heavier elements, such as group IV hydrides, as hydrogen is likely to be 'chemically pre-compressed' in these compounds [5–9]. In fact, in the case of silane SiH_4, several theoretical [10–12] and experimental [13,14] studies have shown that its metalization pressures may be substantially lower than that of pure hydrogen. These hydrogen rich full-shell group IV hydrides can also absorb additional hydrogen at high pressures to form stoichiometric van der Waals compounds such as $CH_4(H_2)_2$, $SiH_4(H_2)_2$ etc. [15,16]. X-ray diffraction experiments by Strobel et al. on $SiH_4(H_2)_2$ showed that it forms a highly symmetrical, well ordered structure above 7 GPa. Raman and IR measurements under pressure showed that vibration frequencies are anti-correlated to pressure, implying H_2 bond weakening at unusually low pressures. They also observed a darkening of the sample at a pressure around 35 GPa, interpreted as indicative of metalization. Studies on the iso-structural compound $SiH_4(D_2)_2$ also revealed a time evolution of Raman spectra, which was interpreted in terms of site exchange between H and D atoms. This implied high proton mobility in this compound which was also speculated to be pressure induced quantum lattice melting [17].

To understand the experimental results better, several theoretical investigations followed. For example, it was shown that the crystal structure of this stoichiometric compound may be a slight distortion of FCC to a tetragonal one, having a slightly elongated *c*-axis [18]. Total energy calculations combined with genetic algorithms have predicted the transformation of this compound to a metallic orthorhombic phase at high pressures. However, the pressure of transformation to this phase is found to be quite high, ∼248 GPa [19,18]. Other theoretical calculations employing different computational schemes predict quite different metalization pressures of this compound viz, 164 and 200 GPa [20,21]. However, the calculations support the existence of a substantial charge density overlap between silane and hydrogen [22]. In spite of the observation of unambiguous anti-correlated behavior of most of the vibration frequencies with pressure [23], several calculations predict only a marginal elongation (<0.01 Å) in the H_2 bond length up to 35 GPa.

Despite a number of theoretical publications, some issues remain unsettled. One of these is the observed darkening of the sample close to 35 GPa. In the absence of metalization, this could also be due to molecular dissociation of silane, catalyzed by metallic gasket and aided by bond softening [24]. None of the studies provide an understanding of the observed H–D exchange. This may be a consequence of the dynamics and hence a quantum molecular dynamics simulation can shed more light into this.

* Corresponding author.
E-mail address: shanavas@barc.gov.in (K.V. Shanavas).
[1] Current address: Department of Physics, University of Missouri, Columbia, MO 65211, USA.

0038-1098/$ – see front matter © 2012 Elsevier Ltd. All rights reserved.
doi:10.1016/j.ssc.2012.02.012

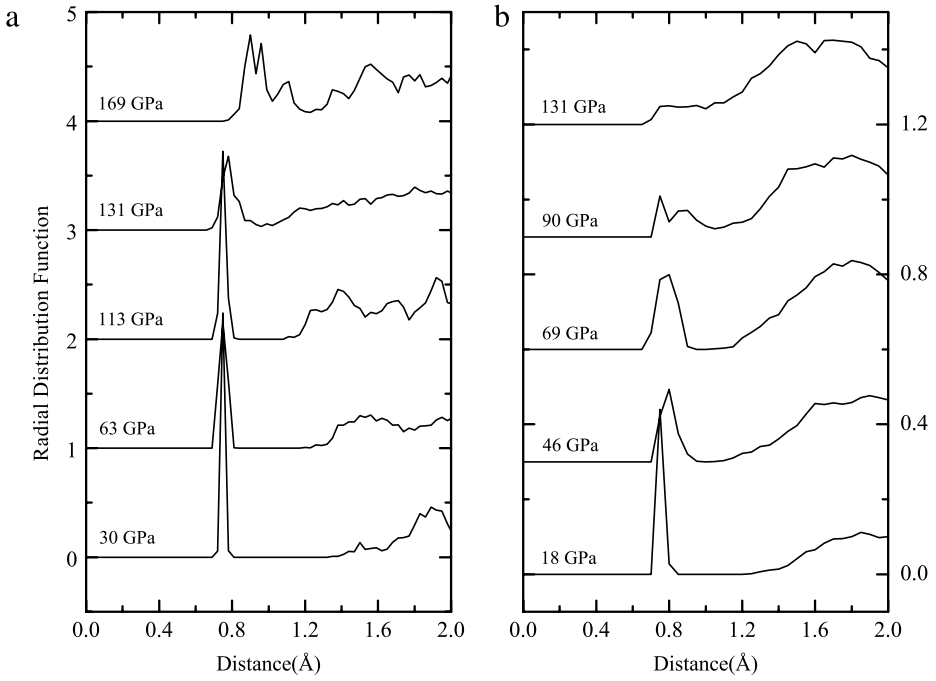

Fig. 1. H–H radial distribution function at a few representative pressures for (a) pure hydrogen (b) $SiH_4(H_2)_2$.

We present in this article, results of first principles calculations, which show a significant softening of H_2 bond beyond ∼40 GPa, brought about by an increased transfer of charge density from bonding to antibonding states. Our quantum MD results show that HD exchange is a consequence of pressure induced weakening of Si–H and H–H covalent bonds and the exchange is a three stage dynamical process involving multiple silane molecules.

This manuscript is organized as follows. We give the details of the computational procedure in Section 2. In Section 3.1 we present our results on pressure induced elongation of H_2 bond, which is explained in terms of computed changes in the charge densities. Temporal evolution of the structure displaying exchange of hydrogen atoms and results of our calculated Raman spectra based on first principles lattice dynamical calculations are given in Section 3.2.

2. Computational method

First principles molecular dynamics simulations are performed within the framework of density functional theory using the VASP package [25,26]. The wave functions are expanded in plane wave basis and exchange correlation effects are incorporated using local density approximation. An important limitation of this approximation is that it does not correctly incorporate the weak van der Waals interactions, that can become significant in the absence of chemical bonding. However, under pressure as molecules come closer and their charge densities overlap, much stronger electronic effects will take over and it can be safely ignored [20].

The ion–electron interactions are described by projector augmented wave potentials (PAW) [27,28]. A cutoff energy of 700 eV and a Monkhorst–Pack mesh of 4 × 4 × 4 are used to obtain highly converged structural properties. Simulations employed a time step of 0.5 fs to integrate the equations of motion under constant volume and Nosé–Hoover thermostat to keep temperature constant. Equilibration runs are typically done for 0.5 ps and average quantities are calculated over another 0.5 ps. Phonon dispersion curve and non-resonant Raman scattering intensity calculations have been performed using density functional perturbation theory [29] as implemented in QUANTUM ESPRESSO code [30].

3. Results

A unit cell containing four silane and 8 hydrogen molecules in the FCC lattice of Ref. [17] with a lattice constant of 6.13 Å was used as the starting configuration. Upon structural relaxation at constant volume, this cell is found to have a pressure of 9.3 GPa, which agrees well with the experimental value [17]. The stability of this structure is verified by calculating full phonon dispersion spectrum. We also find that H_2 and SiH_4 molecules are free to rotate in the structure, confirming earlier observations [19,23].

3.1. H_2 bond strength under pressure

Volume of a well equilibrated simulation cell containing $SiH_4(H_2)_2$ is reduced gradually, allowing the system to relax for several thousand steps at each volume. The variation of inter particle distances are analyzed by calculating radial distribution functions (RDF) for Si–Si, Si–H and H–H pairs of atoms. The H–H RDF averaged over 100 configurations and at various pressures is given in Fig. 1. A similar plot of RDF for pure molecular hydrogen is also provided, which was calculated starting from a MD cell containing 64 hydrogen molecules and subjecting it to pressures. The figure shows clearly that, the first peak corresponding to bonded hydrogen atoms move to higher values at higher pressures. The figure also shows that the second peak, corresponding to intermolecular H–H distance approaches the first peak and merges with it. In the case of the system containing only H_2 it happens close to 131 GPa, while in the case of $SiH_4(H_2)_2$ this happens close to 46 GPa.

Generally, average bond lengths are calculated by averaging over the distances up to the first minimum in the pair correlation function between bonded atoms. However, this procedure does not take into account the "baseline" caused by nearby molecules and unbound atoms [31]. To avoid this overestimation of bond lengths, we fit each of the H–H pair correlation function to the functional form:

$$g(r) = \lambda g_f(r; c_f, \sigma_f) + (1 - \lambda) g_s(r; c_s, \sigma_s) \quad (1)$$

where g_f and g_s are Gaussians for the first and second neighbor peaks and c and σ are fitting parameters corresponding to center

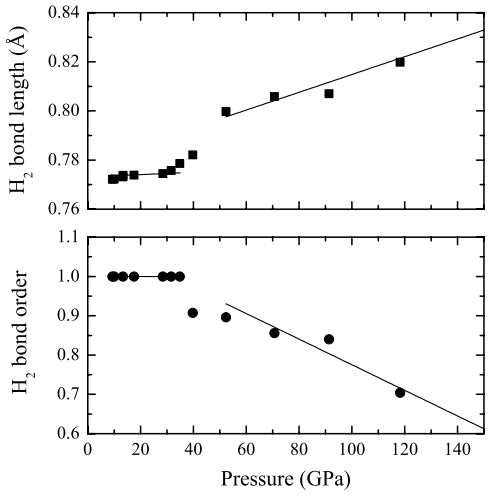

Fig. 2. Variation of H–H bond length and bond order as a function of pressure for $SiH_4(H_2)_2$ solid. Abrupt changes in the behavior are observed between 40 and 50 GPa. Straight lines are guide to the eye.

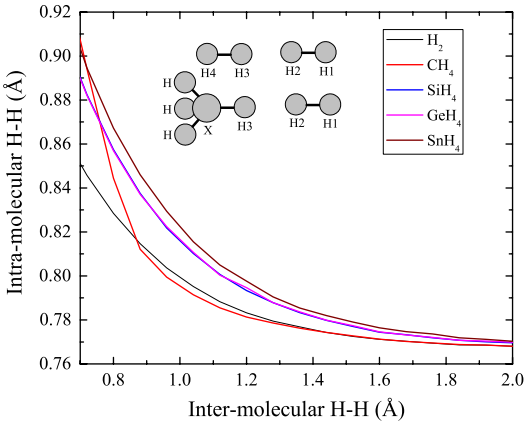

Fig. 3. Variation of bond length of H_2 molecule as a function of intermolecular H–H distance. Arrangement of molecules for the calculation is shown in the inset.

and width of the Gaussian respectively. The parameter λ is the bond order (representative of valency) which gives the fraction of protons that are bound into a molecule; a value of 1 means all H_2 molecules are intact [31]. The most probable value of bond length (c_f) and bond order (λ) are plotted as a function of pressure in Fig. 2.

As we can see, the H_2 covalent bond length and bond order exhibit a change in behavior close to 40 GPa. The volume compression at this pressure (V/V_0) is ∼0.54, which is close to the experimental value of 0.53 [17]. Bond order remains 1 up to 40 GPa, drops abruptly and continues to decrease, indicating that H_2 molecule becoming progressively weaker beyond this pressure. In the case of pure hydrogen, a similar decrease in bond order was observed in the range of 150–200 GPa in earlier studies [31]. This behavior of bond length seems to suggest two regimes (below 40 GPa were variation is almost zero and above 60 GPa where elongation is almost constant) connected by an abrupt increase. It is interesting to note that although a sudden change in bond length and bond order is observed close to 40 GPa, as expected from experiments [17], our calculated band gaps at these pressures reveal the system does not become metallic, which in fact agrees with other theoretical predictions [20,21].

To understand why silane molecules weaken H_2 bond strength, we considered a simple one dimensional model in which two H_2 molecules are placed end-on along z-axis as shown in the inset of Fig. 3. We then varied H_2 non bonded distance (d_{nbo} between

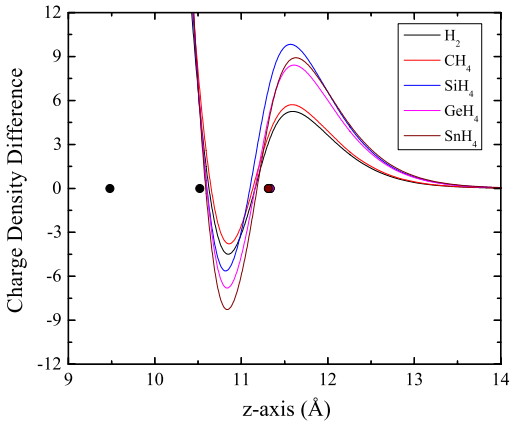

Fig. 4. One dimensional charge density differences induced on a hydrogen molecule by another molecule placed next to it. Filled circles represent hydrogen atoms.

H3–H2) by constraining the positions of adjacent hydrogen atoms and monitored the H_2 bond length (d_{bnd} between H1–H2). The farther atoms (H4 and H1 in the figure) are allowed to relax along the z-axis. The calculations are then repeated by replacing one of the molecules (H4–H2) by XH_4, where X is other known stable variants of IV group elements like C, Si, Ge and Sn with one of the hydrogen atom pointing along the axis as shown in Fig. 3. Although we have approximated the complex three dimensional interactions with multiple neighbors to a single interaction in 1D, we believe this model to be a reasonable representation of the real system for providing essential insights. In fact, this simple model does predict SiH_4 to have a higher effect than H_2 as expected. It also predicts SnH_4 to have higher bond weakening effect and hence might be more effective in bringing about metalization in hydrogen. However, this model does not take into account the molecular rotations present in the FCC structure. In fact, the two regimes present in the variation of bond length of Fig. 2 is a consequence of SiH_4 and H_2 molecules rearranging to avoid reducing intermolecular distances substantially. Beyond the critical pressure of about 40 GPa, the intermolecular distances may become too small leading to increased charge transfer and consequent H_2 bond elongation.

In the case of H_2 in the interstitials of GaAs crystals [32], it was found that the lattice induces charge transfer from bonding to antibonding states which causes elongation of bond length and downward shift of vibrational frequencies. To check this, we calculated the charge density differences (integrated around molecular axis) for the molecular arrangement in Fig. 3 with d_{nbo} fixed at 1 Å. The result, shown in Fig. 4 displays a similar trend. Moreover, the redistribution of charge from bonding to antibonding states is found to be higher when the neighboring molecule is XH_4, instead of H_2. The plots also show substantial overlap of charge density between H_2 and neighboring molecule in agreement with Ref. [22].

Results presented in Fig. 4 also show that the redistribution of charge affects the bond length in two ways: removal of charge from the bonding region reduces the attraction between the bonded nuclei and addition of charge in the antibonding region increases the repulsion; both of which cause the bond to elongate. At the same time, antibonding charge also helps to reduce the repulsion between non bonded nuclei. The figure shows that CH_4 results in lowest reduction in bonding charge density (in fact even lower than H_2), while SnH_4 results in the maximum reduction. Interestingly, the bond elongation also follows the same order as of Fig. 3. According to Fig. 3, both SiH_4 and GeH_4 exhibit similar elongation behavior although Ge clearly has a larger effect on

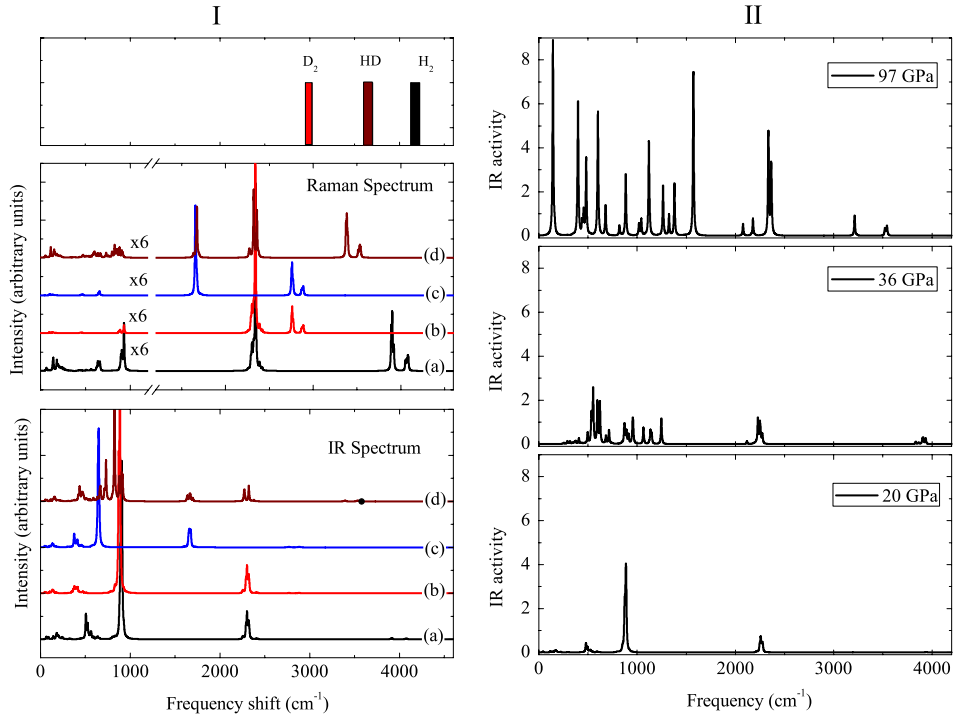

Fig. 5. I. Computed Raman scattering and IR absorption spectra are shown at top and bottom panels respectively for (a) $SiH_4(H_2)_2$, (b) $SiH_4(D_2)_2$, (c) $SiD_4(D_2)_2$ and (d) $SiH_4(HD)_2$. All the spectra are generated by fixing mode width to 5 cm^{-1}. Vertical bars in figure represent the experimentally determined vibration bands of H_2, HD and D_2 II. Computed IR activity of $SiH_4(H_2)_2$ at three representative pressure (shown on same scale).

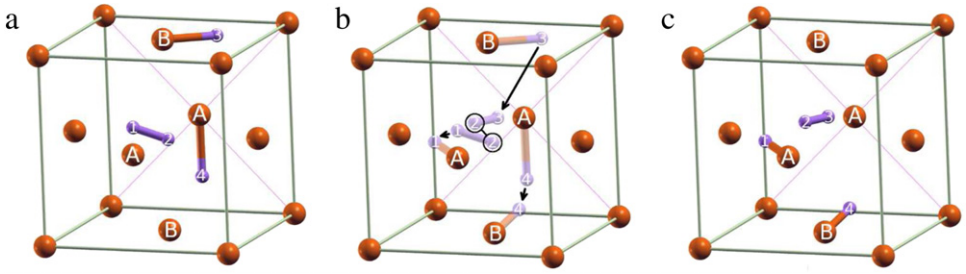

Fig. 6. Hydrogen exchange mechanism (explained in the text) in $SiH_4(H_2)_2$. Note that only hydrogen atoms participating in the event are shown. The back face of the cell is marked by its diagonals and the arrows represent the movement of atoms. A & B, and numbers 1, 2, 3 & 4 represent two silicon and four hydrogen atoms that participate in the event.

bonding density. But SiH_4 has a larger effect on antibonding density which would compensate for the reduced effect on bonding density resulting in similar effect for both the molecules. Our Bader charge analysis [33] shows that hydrogen atoms bonded to Si, Ge and Sn have charges higher than isolated hydrogen atom (1.6e, 1.2e and 1.25e respectively); while hydrogen connected to C has less (0.95e) which may also explain the observed behaviors, mentioned above.

3.2. Hydrogen exchange under pressure

The Raman spectrum of $SiH_4(D_2)_2$ under pressure was found to evolve with time in Ref. [17], interpreted by its authors as a consequence of exchange of H and D between SiH_4 and D_2. To verify this, we computed IR and Raman scattering spectrum of $SiH_4(H_2)_2$, $SiH_4(D_2)_2$, $SiD_4(D_2)_2$ and $SiH_4(HD)_2$ close to 20 GPa which is shown in Fig. 5. Comparison of these spectra with the experimental recorded Raman spectra of the mixture at different elapsed time shows that initially observed spectrum corresponds to $SiH_4(D_2)_2$ while the one recorded after 24 h matches with $SiH_2D_2(HD)_2$, clearly validating the hydrogen exchange. We also computed Raman and IR absorption spectra of $SiH_4(H_2)_2$ at different pressures (20, 36 and 97 GPa) which show that all the modes soften (particularly H_2 stretching mode) with increasing pressure. In addition, we have also observed that IR activity of the most of modes increases with pressure, as shown in Fig. 6.

Instead of carrying out additional calculations for SiH_4 and D_2 mixture, we tagged hydrogen atoms to track their temporal evolution. The dynamical simulations show that at 300 K, hydrogen exchange between silane and hydrogen molecules takes place only above ~90 GPa. At lower pressures the process requires elevated temperatures, indicating the presence of a kinetics barrier which reduces under pressure and disappears at 90 GPa. Our simulations also show that hydrogen exchange takes place in three steps: (1) a transition state is formed by the transfer of hydrogen between two adjacent SiH_4 molecules forming a SiH_3 and SiH_5, (2) the H_2 molecule dissociates and one hydrogen atom moves to the SiH_3, while (3) SiH_5 donates a hydrogen atom which combines with the hydrogen atom to form H_2. The three distinct stages in the process are depicted pictorially in Fig. 6.

Fig. 7 depicts the temporal evolution or the dynamics of the process. We have plotted the relevant bond lengths between four

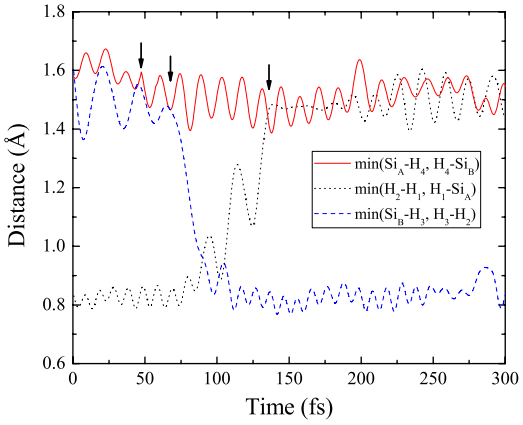

Fig. 7. Evolution of bond distances as a function time in the hydrogen exchange process at 90 GPa and 300 K. Bond breaking/formations are marked by arrows. The exchange process starts around 50 fs and is completed before 125 fs and the system equilibrates beyond it.

hydrogen and two silicon atoms that take part in the process. The three steps mentioned earlier are marked by arrows in the plot. We see that the process initiates when H_4 leaves Si_A around 50 fs after the beginning of the simulations, marked by the first arrow. Beyond the second arrow (75 fs) it is attached to the second silicon Si_B. At this moment Si_A is hydrogen deficient and Si_B is hydrogen rich. As one would expect, immediately after H_4 attaches to Si_B, one of its bonds (H_3) starts weakening. Around 125 fs, marked by the third arrow, the hydrogen molecule donates a hydrogen to the deficient silane Si_A and H_3 detaches completely from Si_B to form H_2 molecule back.

Hence, the exchange is initiated by transfer of hydrogen between to silane molecules. At 90 GPa distance between Si atoms on adjacent face centers (A and B) is 3.3 Å, which is small enough (Si–H distance at this pressure is 1.6 Å) to allow hydrogen transfer between them without large thermal activation. Hence, according to our simulations the hydrogen exchange is a dynamical process, expedited by elongation of bond lengths and reduction in volume. Inclusion of zero point energy (ZPE) will reduce the pressure at which this exchange takes place. Experimental observation of H–D exchange at low pressure may also be due to large experimental time scales or catalysis by gasket as speculated by the authors of Ref. [17].

4. Conclusions

Our ab-initio calculations on $SiH_4(H_2)_2$ in the FCC lattice show that pressure causes substantial elongation of H_2 bond length above 40 GPa. In contrast to earlier simulations that predicted marginal elongation of hydrogen bond length, these results indicate that dynamics play a vital role in the high pressure properties of this compound. Transfer of charge from bonding to antibonding states is responsible for the elongation and our studies indicate that $SnH_4(H_2)_2$ interaction may be more effective in bringing about this transition. HD exchange has been confirmed as the reason for observed variation of Raman spectra and dynamics of the process indicate it to be a three step process. An activation barrier prevents the exchange from taking place at room temperature in simulations below 90 GPa, which may be reduced by the incorporation of ZPE.

Acknowledgments

We thank S.K. Sikka for critical reading of the manuscript and several suggestions. We also acknowledge K.K. Pandey for several illuminating discussions, T.A. Strobel, M. Somayazulu and Indra Dasgupta for valuable feedback. The calculations were carried out on PLUTO parallel computing facility in Bhabha Atomic Research Centre.

References

[1] E. Wigner, H.B. Huntington, J. Chem. Phys. 764 (1935) 3.
[2] E. Babaev, A. Sudbo, N.W. Ashcroft, Nature 431 (7009) (2004) 666.
[3] K.A. Johnson, N.W. Ashcroft, Nature 403 (2000) 632.
[4] M.S.R.M. Martin, Phys. Rev. Lett. 84 (2000) 6070.
[5] N.W. Ashcroft, Phys. Rev. Lett. 92 (2004) 187002.
[6] N.W. Ashcroft, Phys. Rev. B 41 (1990) 10963.
[7] G. Gao, A.R. Oganov, A. Bergara, M. Martinez-Canales, T. Cui, T. Iitaka, Y. Ma, G. Zou, Phys. Rev. Lett. 101 (2008) 107002.
[8] M. Martinez-Canales, A.R. Oganov, Y. Ma, Y. Yan, A.O. Lyakhov, A. Bergara, Phys. Rev. Lett. 102 (2009) 087005.
[9] G. Gao, A.R. Oganov, P. Li, Z. Li, H. Wang, T. Cui, Y. Ma, A. Bergara, A.O. Lyakhov, T. Iitaka, G. Zou, Proc. Natl. Acad. Sci. USA 107 (4) (2010) 1317–1320.
[10] J. Feng, W. Grochala, T. Jaron, R. Hoffmann, A. Bergara, N.W. Ashcroft, Phys. Rev. Lett. 96 (2006) 017006.
[11] Y. Yao, J.S. Tse, Y.M.K. Tanaka, Eur. Phys. Lett. 78 (2007) 37003.
[12] D.Y. Kim, R.H. Scheicher, S. Lebegue, J. Prasongkit, B. Arnaud, M. Alouani, R. Ahuja, Proc. Natl. Acad. Sci. USA 105 (2008) 16454.
[13] X.J. Chen, V.V. Struzhkin, Y. Song, A.F. Goncharov, M. Ahart, Z. Liu, H.K. Mao, R.J. Hemley, Proc. Natl. Acad. Sci. USA 105 (2008) 20.
[14] M.I. Eremets, I.A. Trojan, S.A. Medvedev, J.S. Tse, Y. Yao, Science 319 (2008) 1506.
[15] S. Wang, H. Mao, X.J. Chen, W.L. Mao, Proc. Natl. Acad. Sci. USA 106 (2009) 14763.
[16] M.S. Somayazulu, L.W. Finger, R.J. Hemley, H.K. Mao, Science 271 (1996) 1400.
[17] T.A. Ströbel, M. Somayazulu, R.J. Hemley, Phys. Rev. Lett. 103 (2009) 065701.
[18] Y. Li, G. Gao, Q. Li, Y. Ma, G. Zou, Phys. Rev. B 82 (2010) 064104.
[19] Y. Li, G. Gao, Y. Xie, Y. Ma, T. Cui, G. Zou, Proc. Natl. Acad. Sci. USA 107 (2010) 15708.
[20] M. Ramzan, S. Lebègue, R. Ahuja, Phys. Rev. B 81 (2010) 233103.
[21] X.-Q. Chen, S. Wang, W.L. Mao, C.L. Fu, Phys. Rev. B 82 (2010) 104115.
[22] K. Michel, Y. Liu, V. Ozolins, Phys. Rev. B. 82 (2010) 174103.
[23] W.-L. Yim, J. Tse, T. Iitak, Phys. Rev. Lett. 105 (2010) 215501.
[24] O. Degtyareva, J. Proctor, C.L. Guillaume, E. Gregoryanz, M. Hanfland, Solid State Commun. 149 (2009) 1583.
[25] G. Kresse, J. Hafner, Phys. Rev. B 47 (1993) R558.
[26] G. Kresse, J. Furthmüller, Phys. Rev. B 54 (1996) 11169.
[27] P.E. Blöchl, Phys. Rev. B 50 (1994) 17953.
[28] G. Kresse, D. Joubert, Phys. Rev. B 59 (1999) 1758.
[29] M. Lazzeri, F. Mauri, Phys. Rev. Lett. 90 (2003) 036401.
[30] P. Giannozzi, S. Baroni, N. Bonini, M. Calandra, R. Car, C. Cavazzoni, D. Ceresoli, G.L. Chiarotti, M. Cococcioni, I. Dabo, A.D. Corso, S. Fabris, G. Fratesi, S. de Gironcoli, R. Gebauer, U. Gerstmann, C. Gougoussis, A. Kokalj, M. Lazzeri, L. Martin-Samos, N. Marzari, F. Mauri, R. Mazzarello, S. Paolini, A. Pasquarello, L. Paulatto, C. Sbraccia, S. Scandolo, G. Sclauzero, A.P. Seitsonen, A. Smogunov, P. Umari, R.M. Wentzcovitch, J. Phys. Condens. Matter 21 (2009) 395502.
[31] K. Delaney, C. Pierleoni, D. Ceperley, Phys. Rev. Lett. 97 (2006) 235702.
[32] Y. Okamoto, A. Oshiyama, Phys. Rev. B 56 (1997) R10016.
[33] G. Henkelman, A. Arnaldsson, H. Jónsson, Comput. Mater. Sci. 36 (2006) 254.